Available online at www.sciencedirect.com
ScienceDirect
Cement & Concrete Composites 28 (2006) 898–905
Cement & Concrete Composites
www.elsevier.com/locate/cemconcomp

Ductility of FRP plated flexural members

Deric John Oehlers *

School of Civil and Environmental Engineering, The University of Adelaide, Adelaide, SA 5005, Australia

Available online 1 September 2006

Abstract

The design of reinforced concrete (RC) flexural members such as beams, slabs and columns is intrinsically based on the inherent ductility of the member. In reinforced concrete beams and slabs, ductility is generally achieved by using 'under-reinforced' sections and generally governed by the neutral axis depth parameter k_u which requires ultimate failure by concrete crushing at a specified strain ε_c. As the plates of fibre reinforced polymer (FRP) plated RC beams can fracture or debond before the concrete crushes at ε_c, the k_u approach is not directly applicable. Hence, new fundamental approaches and a deeper understanding of ductility are required which are the subjects of this paper.

Keywords: FRP; Ductility; Reinforced concrete; Flexure

1. Introduction

Reinforced concrete structural engineers have long known the importance of ductility in the static design of frames. Often, reinforced concrete frames are analysed elastically and designed plastically and this apparent disparity is accommodated through ductility or rotation in sections. Ductility is, therefore, an inherent part of the design procedure even though it is intrinsically incorporated or hidden within national standards or codes in the design for strength. Ductility is essential in allowing the structure to achieve its ultimate strength as governed by sectional strengths and is obviously important in seismic and blast loadings where the ability to absorb energy is of prime importance.

Ductility is an extremely complex problem even for unplated reinforced concrete beams where concrete crushing at ε_c always controls failure, let alone for FRP plated structures where either concrete crushing, or plate fracture or plate debonding can now control the failure and, hence, the ductility. The fundamental principles governing the ductility of unplated RC beams will first be considered as this forms the foundation for an ensuing section on a fundamental discussion of the more complex problem of the ductility of FRP plated RC flexural members. The long term objective is to develop generic ductility rules that encompass all types and forms of plated and unplated structures which will allow plating to become a viable retrofitting option for most circumstances.

2. Ductility of unplated RC beams

2.1. Classical problem

Let us consider the encastre beam in Fig. 1(a) that is subjected to a uniformly distributed load that induces a static moment M_{stat} and which has a constant flexural rigidity EI as shown [1]. From linear elastic theory, the support moment $M_{sup} = 2/3M_{stat}$ as shown as line A in Fig. 1(b). This distribution of moment ensures that the slope at the support due to the static moment $(dy/dx)_{stat}$ in Fig. 1(c) is equal to the slope at the support due to the support moment M_{sup} that is $(dy/dx)_{sup}$ in Fig. 1(d).

The elastic distribution of moment, line A in Fig. 1(b), does not require any ductility. If it is necessary to alter the shape of this moment distribution, that is change the ratio of the support moment to sagging moment M_{sup}/M_{sag}

* Tel.: +61 8 8303 5451; fax: 61 8 8303 4359.
E-mail address: doehlers@civeng.adelaide.edu.au

0958-9465/$ - see front matter © 2006 Elsevier Ltd. All rights reserved.
doi:10.1016/j.cemconcomp.2006.07.006

Nomenclature

CDC	critical diagonal crack
CFRP	carbon FRP
D	disturbed region
d	effective depth of beam
ds/dx	slip strain
EB	externally bonded
EI	flexural rigidity
EI_{db}	secant flexural rigidity at plate debonding
FRP	fibre reinforced polymer
IC	intermediate crack
k_u	neutral axis depth factor
L	length of shear span
L_{hin}	hinge length
M	moment
M_{cap}	moment capacity
M_{max}	position of maximum moment
M_{stat}	static moment
M_{sag}	sagging moment
M_{sup}	support moment
NSM	near surface mounted
PE	plate end
s	slip
UD	undisturbed region
w	crack width
z	length hogging or −ve region
ΔM_{stat}	increase in static moment
$\Delta\chi$	step change in curvature
ε_c	concrete crushing strain
ε_{tf}	strain at tension face
ε_{fi}	full-interaction strain profile
ε_{pi}	partial-interaction strain profile
θ	rotation
χ	curvature
χ_{cap}	curvature at M_{cap}
χ_e	elastic curvature
χ_h	curvature in hinge

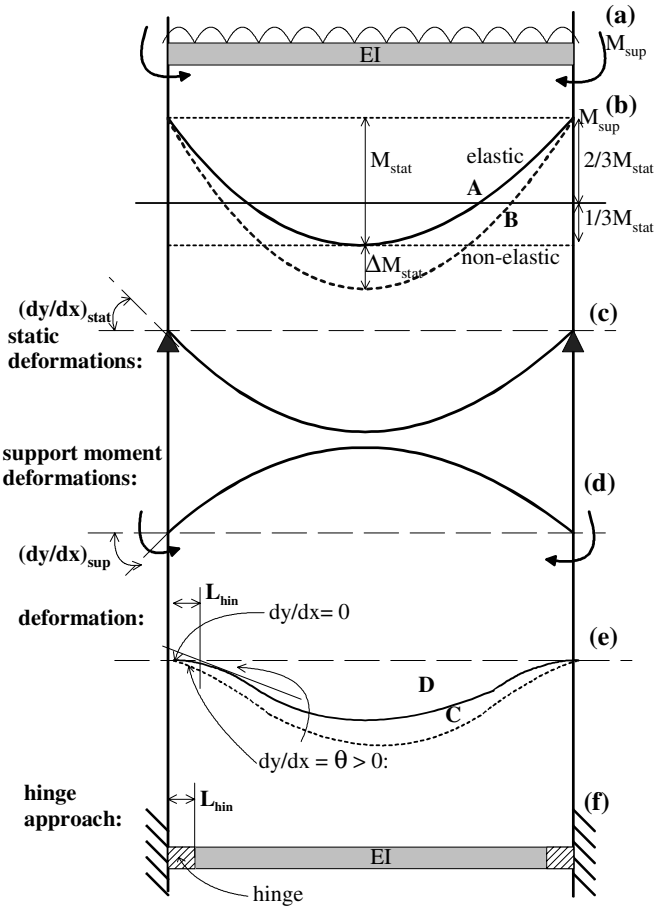

Fig. 1. Hinge concept.

from its elastic value of 2:1, for this specific case of an encastre beam, then ductility is required. Take for example the moment distribution line B in Fig. 1(b) where the sagging moment has increased by ΔM_{stat}. This non-elastic distribution of moment represents the condition where the gradual increase in the applied load has caused the support moment capacity to be reached first so that any further increase in the static moment is taken up by an increase in the sagging moment. No longer is the support to sagging moment ratio equal to 2:1 and, therefore, no longer is $(dy/dx)_{stat}$ in Fig. 1(c) equal to $(dy/dx)_{sup}$ in Fig. 1(d). Hence, there is an apparent discontinuity in the slope at the support which is referred to as the rotation $\theta = (dy/dx)_{stat} - (dy/dx)_{sup}$ which is shown as line C in Fig. 1(e). The rotation θ is often assumed to be accommodated within a small region of the beam of length L_{hin} as shown in Fig. 1(f) where the change in slope between the extremities of the hinge equals θ as in line D in Fig. 1(e). Hence, the slope at the support end of the hinge is still zero so that the concept of a discontinuity of slope at the support is really only a mathematical convenience.

The problem is in quantifying the length of the hinge L_{hin} in Fig. 1(f) and this seemingly intractable problem was first recognised way back in the nineteen-sixties by Johnson, Barnard and Wood [2–5]. Let us consider a uniformly loaded encastre beam as in Fig. 1(a) that has a sectional moment (M) curvature (χ) relationship as shown in line O–P–A Fig. 2 that has: an initial elastic flexural rigidity EI along O–P; a moment capacity M_{cap} at a curvature χ_{cap}; and a falling branch plateau P–A as shown. As the beam is gradually loaded, it remains elastic at a flexural rigidity EI until it reaches its moment capacity M_{cap}. The distribution of moment and curvature is shown as lines A in Fig. 3(a) and (b), where at a point at the support the moment is M_{cap} and the curvature is M_{cap}/EI and elsewhere the moment

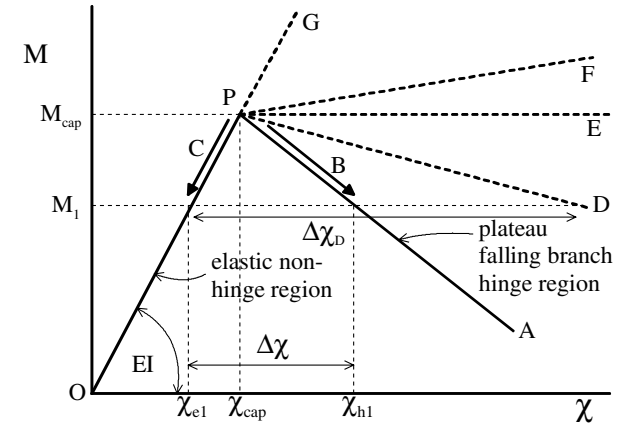

Fig. 2. Moment/curvature plateaus.

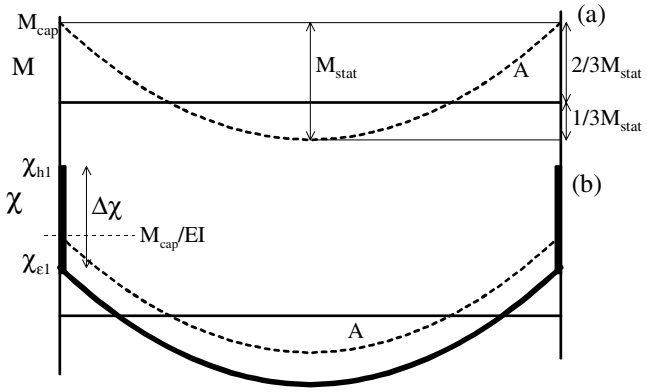

Fig. 3. Curvature distribution.

and curvature is less. As the applied load is further increased, the moment at the support at the point at which M_{cap} was achieved reduces along the falling branch as shown by the arrow B in Fig. 2 and immediately adjacent to this point the moment reduces along the elastic region as shown by the arrow C. Hence at some arbitrary support moment M_1, the curvature in the point at which M_{cap} had been achieved is χ_{h1} and that in the immediately adjacent elastic section of the beam is χ_{e1}. It has been shown that the hinge occurs at a point, therefore, the hinge length L_{hin} is of zero length and within this hinge length of zero length, there is a step change in curvature of $\Delta\chi = \chi_{h1} - \chi_{e1}$ as shown in Fig. 3 which is in practice impossible.

The original solution to this dilemma proposed by Barnard and Johnson [2] was to assume a finite hinge length. However, it should be remembered that their original solution was based on the assumption that the concrete had crushed, as the concrete crushing region requires in reality a finite length. It can be shown in Fig. 2 that using a less steep falling branch plateau as in line P–D only increases the step change in the curvature to $\Delta\chi_D$ and it can also be deduced that the same problem of zero hinge length also applies to a horizontal plateau as in line P–E. For plateaus with rising branches such as line P–F, there is a theoretical solution for the hinge length which can be defined as the region of the beam where M_{cap} is exceeded and the properties of the rising plateau govern. However, it is felt that this is unrealistic for two reasons: as line P–F tends to line P–E the hinge length must tend to zero; furthermore as line P–F tends to the elastic case of line P–G, the length of the hinge increases but for the elastic case there must be zero hinge length which is a contradiction. Hence a rising plateau does not provide the correct solution for the hinge length. It may also be worth noting that an analogous problem often occurs in the finite element simulation of the hinge length because the stress/strain relationship of concrete has a falling branch. As an element of concrete crushes and follows its falling branch increasing its strains, the adjacent element remains elastic with reduced strains so that the hinge length is simply the chosen width of the finite element and is not being simulated by the finite element analysis. The question is what is happening and a solution has been sought through numerical modelling.

2.2. Numerical modelling

Partial-interaction numerical models [5–9] have been developed in order to gain an understanding of the behaviour of reinforced-concrete hinges. These models often use a shooting method of analysis [10] that requires the determination of the boundary conditions and, hence, are the first step in developing the governing mathematical equations. Partial-interaction analyses were first developed for composite steel and concrete beams [10,11] to allow for the slip between the concrete and steel elements. However, the problem of simulating the partial-interaction behaviour of reinforced concrete hinges is much more complex than that in composite steel and concrete beams. This is because it is difficult to characterise the boundary conditions, as there may be several layers of reinforcing bars all slipping through the concrete and flexural cracking is a progressive phenomena so that the boundaries keep changing.

The partial-interaction problem is illustrated in Fig. 4 [5]. The hinge may be defined as the region of the beam between sections in which there is full-interaction. Full-interaction being defined as when there is a single linear strain profile such as at ε_{fi}. Between these full-interaction sections there is a step change in the strain profile as shown by ds/dx in the strain profile ε_{pi} due to the slip between the reinforcing bars and the concrete which must occur at least in the vicinity of each flexural crack. The numerical model has also to cope with the disturbed region D where linear strain profiles do not occur.

There has been a gradual and logical progression in finding a solution to this complex problem. The problem was first simplified by treating each block between flexural cracks in Fig. 4 as discrete and independent elements. Numerous boundary conditions have been used to find a solution [6–9] such as: full-interaction at the cracked section; equally spaced cracks; and zero slip mid-way between cracks. The next step was to allow for interaction between

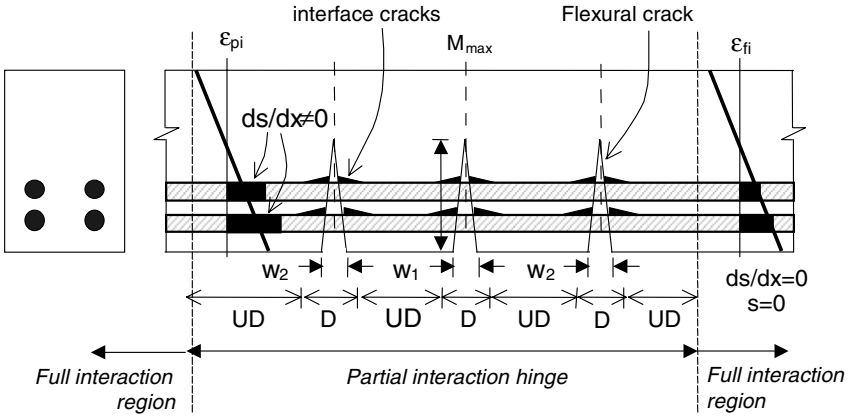

Fig. 4. Partial-interaction hinges.

adjacent elements [5] and this required additional boundary conditions such as the assumption that the crack width varied linearly and the crack faces moved as rigid bodies. These numerical models can be used to simulate the complex behaviour of hinge regions and, hopefully, eventually allow the behaviour of hinges to be quantified for use in design. What has emerged so far is that partial-interaction, that is slip of the reinforcing bars, is beneficial as it makes the whole system more ductile, but at the same time it makes it much more complex in trying to quantify the hinge length and ductility or change in the flexural rigidity EI.

2.3. Mathematical solutions

The ability to redistribute moment which is a measure of the ductility of a beam is usually governed in national codes or standards by the neutral axis depth factor k_u which is the depth to the neutral axis from the compression face as a proportion of the effective depth of the beam d. For convenience, it is often assumed in the analysis of the hinge that the curvature is constant along the hinge length L_{hin} [12]. Hence, the maximum rotation of the hinge $\theta = L_{hin}\chi_{cap}$ where χ_{cap} is the curvature at maximum moment as shown in Fig. 2. Reinforced concrete beams virtually always fail by concrete crushing at ε_c. Therefore, $\chi_{cap} = \varepsilon_c/k_u d$ so that $\theta = L_{hin}\varepsilon_c/k_u d$. It is often assumed that L_{hin} is proportional to d so that θ is proportional to ε_c/k_u. Hence if the concrete crushing strain ε_c is fairly constant, and it is usually assumed to be constant, then θ is inversely proportional to the neutral axis depth parameter k_u. It can now be seen that the k_u approach should only be used when concrete crushing governs failure. Furthermore, it is based on the assumption that the hinge length is a function of the effective depth of the beam. Since Barnard and Johnson's [2] proposition of a finite hinge length, there has been much research on experimentally quantifying the hinge length [13–15] where it has been found that it depends not only on the effective depth of the beam d but also on the distance to the point of contraflexure z.

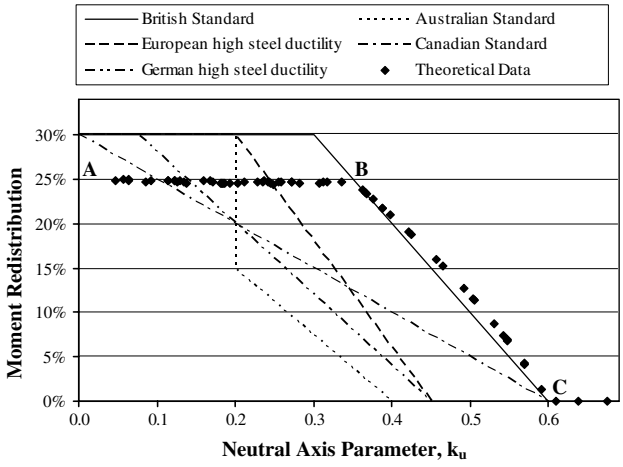

Fig. 5. k_u approach.

Example of the k_u values used in moment redistribution from various national standards are shown in Fig. 5 [16–20]. There would appear to be a wide divergence in values used which may be a reflection of the uncertainty associated with defining the hinge length. What is not often understood is that it can be shown [12] that the horizontal plateau such as A–B is defined by ductile beams that achieve their maximum moment capacities through redistribution. Furthermore, the focal point C is given by a balanced section analysis and it is only the sloping branch B–C where lack of ductility governs.

3. Ductility of FRP plated beams

3.1. Problem

The effect of premature plate debonding or plate fracture on the ability to redistribute moment is illustrated in Fig. 6 using the k_u approach. For convenience in this illustration it has been assumed that the concrete crushes at a fixed strain $\varepsilon_c = 0.0035$. However, this point on the strain profile may reduce and move to the left when plate

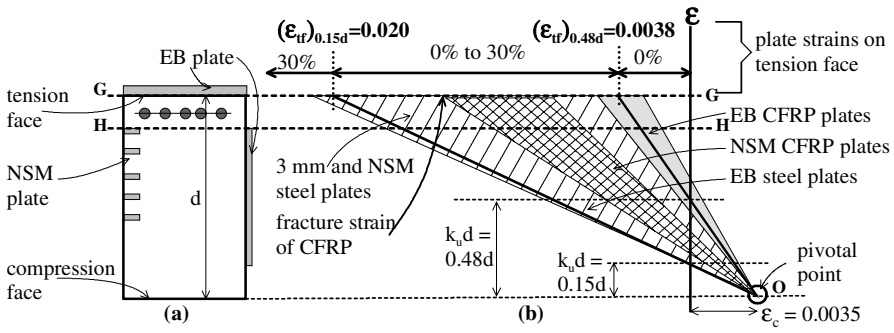

Fig. 6. Affect of plate strains on ductility.

debonding or fracture precedes concrete crushing and, hence, this analysis is only meant as an illustration. From the various k_u approaches shown in Fig. 5, the mean value of k_u equals 0.15 for 30% redistribution and 0.48 for 0% redistribution. The strain profiles based on ε_c and these values of k_u are drawn in Fig. 6. It can be seen that the strain required at the tension face ε_{tf} is independent of the depth of the beam d. Furthermore, the tension face strain required to achieve 30% redistribution is 0.020 and the tension face strain must be greater than 0.0038 to achieve any degree of moment redistribution.

These moment redistribution strains in Fig. 6 described in the previous paragraph have been compared with the range of experimental plate debonding strains [1,21]. Externally bonded (EB) carbon (C) FRP plates tend to debond around the strain of 0.0038 so that moment redistribution is unlikely to occur and, hence, often not allowed in existing guidelines. Thin EB plates and near surface mounted (NSM) steel plates can debond at strains greater than 0.020 so they can accommodate large amounts of moment redistribution. NSM CFRP plates can debond at high strains and can also fracture prior to debonding and so can achieve significant amounts of redistribution as has been shown experimentally [21] and also illustrated in Figs. 7 and 8 for two span continuous beams that were strengthened over the central support with NSM CFRP plates. In Fig. 7 the slab type section had been strengthened with NSM CFRP plates on the tension face and in Fig. 8 the beam type section had been strengthened with NSM CFRP plates on the sides. Both FRP plated beams exhibit large amounts of deformation and, hence, ductility which allowed substantial moment redistribution [21]. It is also worth noting in Fig. 6 that NSM and EB side plates allow larger strains in the tension face and, hence, more moment redistribution and its associated ductility.

It has been shown in the previous section on unplated RC beams that the commonly used and convenient neutral axis depth approach k_u is based on the concrete crushing at ε_c. Hence, the k_u approach can be used for plated structures that fail through concrete crushing before plate debonding or plate fracture. However, the governing failure mode for plated structures is often plate fracture or plate debonding due to intermediate crack (IC) debonding, critical diagonal crack (CDC) debonding or plate end (PE) debonding [1]. Hence an additional or alternative approach for ductility and moment redistribution is required that encompasses both plated and unplated structures. An insight into the behaviour of plated beams is given by numerical simulations.

3.2. Numerical modelling

The numerical simulation of the hinge region of unplated reinforced concrete structures [5] using the shooting method of analysis can be used to analyse the plated hinge region [22]; the difference being the interface shear/slip bond characteristics, which for plates tends to be brittle compared with that of the reinforcing bars. The analyses can be used to quantify the variation in flexural rigidity

Fig. 7. Continuous beam with tension face NSM CFRP plates.

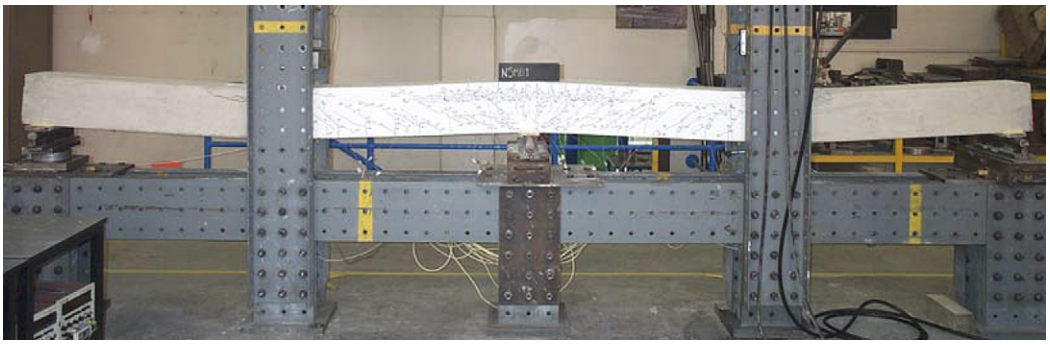

Fig. 8. Continuous beam with side face NSM CFRP plates.

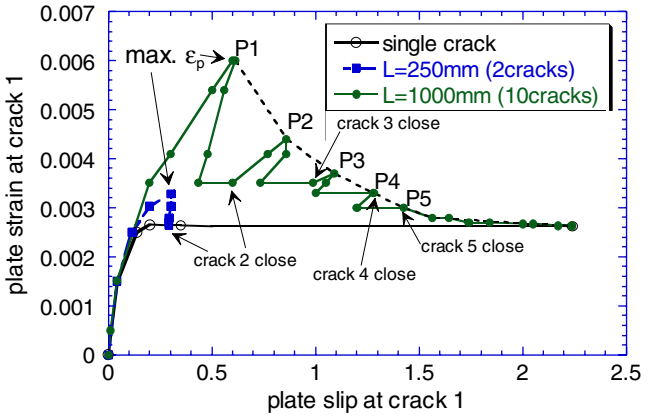

Fig. 9. Debonding strains.

with flexural cracking and should provide an insight into the gradual formation of the plated hinge in order to quantify the hinge characteristics.

An example of a partial-interaction numerical simulation of a plated simply supported beam is seen in Fig. 9. The first flexural crack, *crack 1*, occurs at the position of maximum moment. The ordinate is the plate strain adjacent to *crack 1* and the abscissa the plate slip at *crack 1*. The analysis for a beam with a *single crack* also represents the behaviour of a pull-test with sufficient plate anchorage to achieve its maximum strain. The analysis for a beam with two cracks in a shear span of length $L = 250$ mm represents a beam subjected to high shear forces; it can be seen that the debonding strain is slightly larger than that from the 'pull-tests' that is the beam with a single crack. The analysis of a beam with $L = 1000$ mm and with 10 flexural cracks in the shear span shows that large strains can be achieved but as the plate debonds between flexural cracks the debonding strains reduce until the debonding strain tends to that in a pull-test. It can also be seen in Fig. 9 that the numerical simulation allows for crack closure where necessary.

Already these analyses [23] have shown that the intermediate crack resistance from a fully anchored pull-test is equal to or a lower bound to that in a beam so that the ductility of plated beams can be significantly greater than that anticipated from the debonding strains from pull-tests. However the problem is complex. For example, reinforced concrete beams subjected to large shear forces and those subjected to very low shear forces debond at the IC debonding resistance from pull tests and between these two extremities of vertical shear the IC debonding resistance in beams can be greater than that from pull-tests.

3.3. Mathematical solutions for all failure mechanisms

The hinge approach is mathematically convenient but the problem has always been the quantification of the hinge length which is assumed to depend on such parameters as the depth of the section and the length of the shear span. Furthermore, it is also invariably assumed that the hinge is of a constant length which may be appropriate when the concrete crushes, but which is inconvenient under other circumstances such as at plate debonding at low strains when the beam can be assumed to be elastic in which case there is no moment redistribution so that the slope at the support is zero as in line D in Fig. 1(e), hence, the hinge is of zero length that is it does not exist. It may be more appropriate to assume a variable hinge length for plated structures. Pilot studies [12] suggest that the hinge length increases as moment redistribution increases. Take for example the distribution of moment in Fig. 10 in an encastre beam. For an applied static moment M_{stat}, the elastic support moment is M_{sup}. If moment redistribution requires a support moment $(M_{sup})_{redis}$, then it is suggested [12] that the hinge length is $(L_{hin})_{var}$. Hence at zero moment redistribution, the hinge $(L_{hin})_{var}$ is of zero length and gradually increases in length as redistribution increases. This

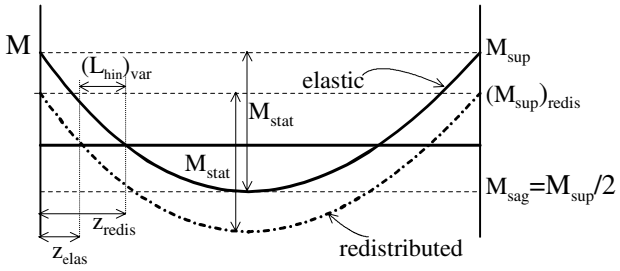

Fig. 10. Variable hinge length.

approach allows the development of a neat mathematical solution for the curvature capacity required for any degree of moment redistribution which can be directly related to the curvature capacity at plate debonding for design.

An alternative to the hinge approach is simply to base the moment redistribution on the variation in the flexural rigidity along the length of the beam [24,25]. This approach is illustrated in Fig. 11 for the case of an encastre plated beam with a point load as in Fig. 11(a). For a given static moment and distribution of moment in Fig. 11(b) and from a full-interaction sectional analysis can be derived the variation in the flexural rigidity in Fig. 11(c). For example the flexural rigidity at the support could be the secant flexural rigidity at plate debonding EI_{db}. For mathematical convenience, it has been assumed that there are linear variations in the flexural rigidity. The variation in curvature is shown in Fig. 11(e) where it can be seen that the curvature still peaks at the support as idealised by the hinge approach. The linear variation in EI in Fig. 11(c) can be idealised as equivalent constant values of EI as in Fig. 11(d) such that the rotation in Fig. 11(e) is the same as that in Fig. 11(f). This is convenient for design, that is the analysis of the beam for ductility, as the beam can now be input as three segments of constant EI within a segment in a stiffness analysis. An iterative approach is required as the positions of the points of contraflexure depend on the differences between the EI values. This linear EI approach correlates well with test results [25] probably because moment redistribution does not depend on the magnitudes of the flexural rigidities but on their proportional differences.

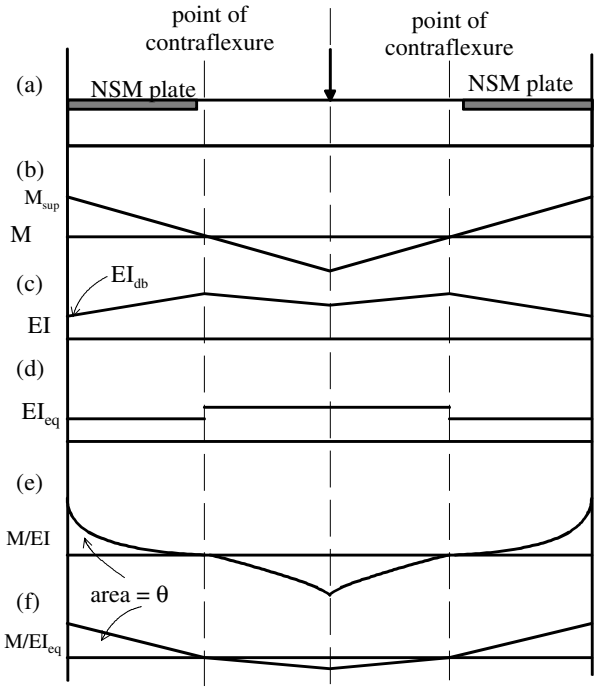

Fig. 11. Moment redistribution by varying EI.

4. Summary

It has been shown that the problem of quantifying ductility in unplated reinforced concrete structures has been an ongoing problem over the last forty years. Compared with unplated reinforced concrete structures in which there is basically one flexural failure mechanism that of concrete crushing, the ductility of plated reinforced concrete structures is much more complex as there are at least two additional failure mechanisms of plate debonding (that includes IC, CDC and PE debonding) and plate fracture. Tests have shown that plated beams can behave in a ductile fashion and redistribute significant amounts of moment, and generic rules are being developed to quantify the ductility in both plated and unplated structures which should significantly expand the use of plating.

References

[1] Oehlers DJ, Seracino R. Design of FRP and steel plated RC structures: retrofitting beams and slabs for strength, stiffness and ductility. Elsevier; 2004.
[2] Barnard PR, Johnson RP. Plastic behaviour of continuous composite beams. Proc Inst Civil Eng 1965;32:161–210.
[3] Barnard PR. The collapse of reinforced concrete beams. In: Flexural mechanics of reinforced concrete. Proceedings of the international symposium, Miami, November. 10–12, 1964. p. 501–11.
[4] Wood RH. Some controversial and curious developments in the plastic theory of structures. In: Heyman J, Leckie FA, editors. Engineering plasticity. Cambridge: Cambridge University Press; 1968. p. 665.
[5] Oehlers DJ, Liu IST, Seracino R. The gradual formation of hinges throughout reinforced concrete beams. Mech Based Design Struct Mach 2005;33:375–400.
[6] Langer P. Verdrehfahigkeit Plastizierter Tragwerksbereiche im Atahlbeton bau. Institu fur Werkstoffe im Bauwesen; Universitat Stuttgart, Report 1987/1, 1987.
[7] Creazza G, Di Marco R. Bending moment-mean curvature relationship with constant axial load in the presence of tension stiffening. Mater Struct 1993;26:196–206.
[8] Fantilli AP, Ferretti D, Iori I, Vallini P. Flexural deformability of reinforced concrete beams. J Struct Eng ASCE 1998:1041–9.
[9] Manfredi G, Pecce M. A refined RC beam element including bond-slip relationship for the analysis of continuous beams. Comput Struct 1998;69:53–62.
[10] Oehlers DJ, Bradford MA. Composite steel and concrete structural members: fundamental behaviour. Oxford: Pergamon Press; 1995.
[11] Newmark NM, Siess CP, Viest IM. Tests and analysis of composite beams with incomplete interaction. In: Proceedings society for experimental stress analysis 1951, 9(1), 1951. p. 75–92.
[12] Oehlers DJ, Campbell L, Haskett M, Antram P, Byrne R. Moment redistribution in RC beams retrofitted by longitudinal plating. Adv Struct Eng 2005;9(2):115–24.
[13] Sawyer HA. Design of concrete frames for two failure stages. Flexural mechanics of reinforced concrete. American Concrete Institute/American Society of Civil Engineers; 1965. p. 405–31.
[14] Corley WG. Rotational capacity of reinforced concrete beams. J Struct Div ASCE 1966;92(ST5):121–6.
[15] Mattock AH. Rotational capacity of reinforced concrete beams. J Struct Div ASCE 1967;93(ST2):519–22.
[16] British Standards Institution. Structural use of concrete – Part 1. BS 8110, 1995.
[17] Canadian Standards Association. Code for the design of concrete structures for buildings. CAN-A23.2, 1994.

[18] Deutsches Institut fur Normung – German Institute of Standards, DIN1045, 1997.
[19] International system of unified standard codes of practise for structures. Model code for concrete structures – Europe. CEB-FIP, 1990.
[20] Standards Australia. Australian concrete structures standard, AS 3600, 1994.
[21] Liu IST, Oehlers DJ, Seracino R. Tests on the ductility of reinforced concrete beams retrofitted with FRP and steel near surface mounted plates. ASCE Compos Construct 2006;10(2):106–14.
[22] Liu IST, Oehlers DJ. Seracino R. Partial interaction numerical simulation of hinges in FRP plated reinforced concrete beams, submitted for publication.
[23] Liu IST, Oehlers DJ, Seracino R, Teng JG. Study of intermediate crack debonding on FRP plated beams. ASCE Compos Construct, in press.
[24] Oehlers DJ, Liu I, Ju G, Seracino R. Moment redistribution in continuous plated RC flexural members. Part 2: flexural rigidity approach. Eng Struct 2004;26:2209–18.
[25] Liu IST, Oehlers DJ, Seracino R. Moment redistribution in FRP and steel plated reinforced concrete beams. ASCE Compos Construct 2006;10(2):115–24.